# Magnetostatic bulk and surface spin-wave focusing in antiferromagnetic thin films

V. Veerakumar and R. E. Camley
*Center for Magnetism and Magnetic Nanostructures, Department of Physics, University of Colorado at Colorado Springs, Colorado Springs, Colorado 80918, USA*

(Received 27 January 2010; revised manuscript received 19 March 2010; published 28 May 2010)

We study the focusing of bulk and surface spin waves in thin antiferromagnetic films. This study is carried out by solving the dispersion relation for the bulk and surface waves to obtain the constant frequency curves in $k$ space (slowness surfaces). The focusing pattern is obtained from the slowness surface by evaluating the curvature at each point on the surface. We have studied the focusing pattern in three uniaxial antiferromagnetic thin films, namely, $MnF_2$, $FeF_2$, and $GdAlO_3$. It is found that the bulk modes in the lower band are focused into a larger number of directions compared to the upper one. The focusing of the bulk modes is stronger when compared to the surface modes. The general trends in the focusing behavior are not affected by changes in anisotropy or exchange fields. However, changes in the frequency or the applied field alter the focusing pattern.

DOI: 10.1103/PhysRevB.81.174432 PACS number(s): 75.30.Ds, 75.50.Ee, 75.70.−i, 85.70.−w

## I. INTRODUCTION

The study of the focusing of phonons in elastic solids had been a topic of considerable interest in the past.[1–7] The important property for a material to exhibit focusing effects is some kind of anisotropy in the system so that the group and phase velocities point in different directions. In the case of elastic solids the phonon focusing occurs due to the inherent anisotropy of the solids. With this in mind one can look for different systems which might exhibit focusing effects.

Recently the present authors studied the focusing of spin waves in thin ferromagnetic films.[8] It was found that in the magnetostatic limit the bulk waves are strongly focused into caustics in four to eight directions which depend on the frequency and applied magnetic field. The surface waves are not as strongly focused as the bulk ones. On the other hand, if the exchange interaction is included in the system the surface waves also become strongly focused, while the focusing behavior of bulk waves is not substantially affected. Further, the focusing directions are tunable with applied field and frequency. Since different external fields cause energy to be focused in different directions, it was proposed that this idea could be used to construct tunable filters and frequency splitters in microwave frequency range.[8]

Also, recently a number of experimental studies have demonstrated focusing effects in ferromagnetic materials.[9,10] One study concentrated on focusing in yttrium iron garnet films where one sees transitions from noncaustic focusing to caustic focusing as the external magnetic field was changed. In a second study focusing effects were seen in metallic Permalloy films where surface spin waves in an extended medium were excited by spin waves in a narrow waveguide. Both studies are in good general agreement with the results in Ref. 8.

The typical frequency of operation for focusing of magnetostatic waves in ferromagnets is in the 1–50 GHz range. If one thinks of devices in the frequency range of the infrared region then one has to choose a different magnetic material. Like the nonreciprocal surface and the backward volume waves in ferromagnets, magnetostatic modes are also known in antiferromagnets. Bulk and surface modes in antiferromagnets have been predicted theoretically and measured experimentally[11–16] in semi-infinite and thin-film geometries. The frequency ranges where the bulk spin waves and the surface waves propagate typically lie somewhere in the infrared region. Also in antiferromagnets one can tune the degree of anisotropy by changing the external field. This clearly shows that we can also expect focusing behavior in antiferromagnets.

With this as background, we study the focusing of the magnetostatic modes in thin antiferromagnetic films in the present paper. It is helpful to first compare the general features of bulk and surface magnetostatic waves in ferromagnetic and antiferromagnetic films. For ferromagnets there is one bulk spin-wave frequency region and at a higher frequency, there is a surface mode. In the case of thin antiferromagnetic films there are generally two bulk spin-wave frequency regions and two surface modes. For both materials the frequency of the bulk and surface waves depends on the direction of propagation and on the magnitude of the wave vector. Furthermore, the phase and group velocities for the magnetostatic modes point in different directions in both materials. So, based on the experience with ferromagnets, it is appropriate to also examine the focusing of the magnetostatic modes in antiferromagnets.

This study is carried out by first solving magnetostatic Maxwell equations in a thin antiferromagnetic film. Then the usual slowness surfaces, which are constant frequency curves in wave-vector space, are obtained by solving the implicit dispersion relation and finally the focusing pattern is obtained from the slowness surface. In the absence of an external field we find that both the bulk and surface modes are focused into caustics. On the other hand when an external field is present, we observe that the bulk modes in the lower frequency band have more focusing directions compared to those in the upper band. Also there is a larger number of focusing directions as the frequency is moved up toward the top of the bulk band. This is similar to the focusing behavior in ferromagnetic thin films. For surface modes, we observe only a weak focusing in the presence of an external field. The focusing directions are tunable by changing the applied field or the frequency. Changes in the exchange field or the anisotropy field modify the frequency of the bulk and surface

 

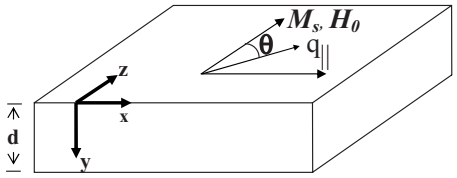


FIG. 1. Geometry of the antiferromagnetic film for calculating the magnetostatic modes. The applied field and the saturation magnetization are in the $z$ direction and parallel to the surface of the film. The uniaxial anisotropy is along the $z$ axis. The wave vector $q_\parallel$ makes an angle $\theta$ with the $z$ direction.

modes and the focusing directions but the general focusing behavior remains the same.

The paper is organized as follows. In Sec. II we obtain the implicit dispersion relation for the magnetostatic modes in antiferromagnetic thin films. The dispersion relation is solved numerically for the magnetostatic modes at different frequencies and applied fields for a 1-$\mu$m-thick $MnF_2$ film, and the focusing patterns are obtained in Sec. III and we conclude our results in Sec. IV.

## II. THEORY

Our approach to this problem is similar to the one we used for ferromagnetic thin films in Ref. 8. The geometry is shown in Fig. 1. The surfaces of the film are parallel to the $x$-$z$ plane, and the film has a thickness $d$. We consider a simple two-sublattice model where the magnetizations in one sublattice is parallel to the $z$ axis and the magnetization in the other sublattice is antiparallel to the $z$ axis. The applied field, $H_0$, is in the $+z$ direction. The spin-wave vector $q_\parallel$ makes an angle $\theta$ with the $z$ axis and lies in a plane parallel to the surfaces. The theory of magnetostatic modes in antiferromagnetic thin films is well known, and hence we only give a brief outline and the necessary equations for our investigation. The complete theory is given in Refs. 15 and 17.

The susceptibility tensor which contains the information about the motion of the spins in the antiferromagnet is given as[15,17]

$$\vec{\chi} = \begin{bmatrix} \chi_a & i\chi_b & 0 \\ -i\chi_b & \chi_a & 0 \\ 0 & 0 & 0 \end{bmatrix}, \tag{1}$$

where

$$\chi_a = \chi^+ + \chi^-, \tag{2}$$

$$\chi_b = \chi^+ - \chi^- \tag{3}$$

with

$$\chi^\pm = \frac{H_A M_s}{H_A(2H_E + H_A) - (\omega/\gamma \pm H_0)^2}, \tag{4}$$

Here $H_A$ is the anisotropy field, $H_E$ is the exchange field, $H_0$ is the external magnetic field, $M_s$ is the saturation magnetization, $\gamma$ is the gyromagnetic ratio, and $\omega$ is the angular frequency.

In the case of large wave vectors we can use the magnetostatic form of Maxwell's equations without retardation as $\nabla \times \mathbf{h} = 0$ and $\nabla \cdot \mathbf{B} = 0$. The first of the given equations is satisfied by the definition of a scalar potential, $\mathbf{h} = -\nabla\phi$. Outside the material, the susceptibility is constant and using the scalar potential in the second of the above equations we can write $\nabla^2\phi = 0$. Inside the material one must use the susceptibility tensor in Eq. (1) which leads to the Walker equation.[18] Seeking solutions of the form $e^{i\mathbf{q}_\parallel \cdot \mathbf{r}_\parallel} e^{iq_y y}$, where $\mathbf{q}_\parallel$ is the wave vector of the magnetostatic mode traveling parallel to the $x$-$z$ plane and $\mathbf{r}_\parallel$ is the position vector where $r_\parallel = x\hat{x} + y\hat{y}$, the Walker equation reduces to

$$(1 + \chi_a)[q_y^2 + q_\parallel^2] - \chi_a q_z^2 = 0. \tag{5}$$

Here the quantity $q_y$ can be real or imaginary describing bulk or surface waves, respectively. Solving Eq. (5) we find that $q_y = \sqrt{q_x^2 + \frac{q_z^2}{(1+\chi_a)}}$, where $q_x = |q_\parallel| \sin\theta$ and $q_z = |q_\parallel| \cos\theta$ are the wave vectors in the $x$-$z$ plane. Here $q_\parallel = \sqrt{q_x^2 + q_z^2}$ and $\theta$ is the angle between the $z$ axis and $q_\parallel$ as shown in Fig. 1. Outside the material one can find that $q_y = -i|q_\parallel|$ for $y < -d/2$ and $q_y = i|q_\parallel|$ for $y > d/2$. With the susceptibilities and potentials one can match the fields inside and outside the material at the boundaries. The boundary conditions require that the potentials and the normal components of $\vec{B}$ should be continuous at $y = \pm d/2$ and on using this we obtain the following dispersion relation for the modes:

$$q_\parallel^2 - q_x^2\chi_b^2 - q_y^2(1 + \chi_a^2) + 2q_\parallel q_y(1 + \chi_a)\cot(q_y y) = 0. \tag{6}$$

The implicit relation in Eq. (6) can be rewritten for the volume and surface modes separately by choosing either real or imaginary value for $q_y$.

In order to study the focusing behavior of the bulk and surface modes we have to solve the dispersion relation in Eq. (6). Since Eq. (6) is an implicit relation we adopt a numerical procedure to solve and study the focusing pattern. The numerical procedure we use here is similar to the one used to study the focusing of phonons[7] and magnons.[8] The key steps involved in the numerical calculations are (i) finding the constant frequency curves or the slowness surfaces in the $q_x$-$q_z$ plane; (ii) finding the normal and curvature "$a$" at every point on the slowness surface. Here the normal describes the direction of energy flow and the magnitude of energy sent in that direction is given by $1/\sqrt{a}$. So when the curvature is zero, it represents a "caustic" meaning that the power flow diverges. However, even without a caustic, one can find substantial focusing of energy, as we will see.

## III. NUMERICAL RESULTS AND DISCUSSION

In this section we solve the implicit dispersion relation in Eq. (6) numerically and find the ensuing focusing patterns. In order that our results could be confirmed experimentally we have used three uniaxial antiferromagnets, $MnF_2$, $FeF_2$, and $GdAlO_3$ for which the parameters are already known[19,20] and are given in Table I.

Before proceeding to the focusing results, we present an example illustrating the magnetostatic spin-wave spectrum in an antiferromagnet. Figure 2 shows the frequency of bulk

TABLE I. The parameters used for different materials in the calculation.

| Material | Exchange field ($H_E$) (kOe) | Anisotropy field ($H_A$) (kOe) | $M_s$ (kOe) |
|---|---|---|---|
| $MnF_2$ | 550 | 7.87 | 0.60 |
| $FeF_2$ | 533 | 197 | 0.56 |
| $GdAlO_3$ | 18.8 | 3.65 | 0.62 |

and surface modes in $MnF_2$ as a function of propagation angle for the case where the thickness to wavelength ratio is given by $q_\parallel d=4$ and for an applied field of $H_0=0.2$ kOe. We note two bulk regions, separated by the surface modes. In the absence of the external field the lower bulk region would be restricted to one particular frequency forming a bulk line instead of a band. Also there are two distinct surface modes even in the absence of the external field. With an external field, the bulk bands are well separated and the two surface modes are further apart in frequency than the zero-field case.

Examples of the shape of the magnetic scalar potential for bulk and surface spin waves propagating at different angles are given in Fig. 3. Figure 3(a) shows the mode pattern for the lowest frequency (pure) bulk mode in the upper bulk band at a frequency of $\omega/\gamma=93.95$ kOe. The lowest bulk mode in the lower bulk region for the frequency of $\omega/\gamma=93.28$ kOe is shown in Fig. 3(b). Figures 3(c) and 3(d) show the upper and lower surface modes at frequencies $\omega/\gamma=93.9$ kOe and $\omega/\gamma=93.48$ kOe, respectively. Figure 3(e) shows a higher order bulk mode at $\omega/\gamma=94.05$ kOe in the upper bulk band region exhibiting a standing wave pattern. The calculations here are for $d=1$ $\mu$m and $q_\parallel$ is allowed to vary in magnitude so that the frequency can remain constant.

In the present study we analyze the focusing patterns of surface and bulk modes in both upper and lower regions in $MnF_2$. Also to study the effect of anisotropy and exchange field on focusing behavior of the bulk and surface modes we have compared our results for $MnF_2$ with those for $FeF_2$ which has a higher anisotropy field and for $GdAlO_3$ which has a lower exchange field.

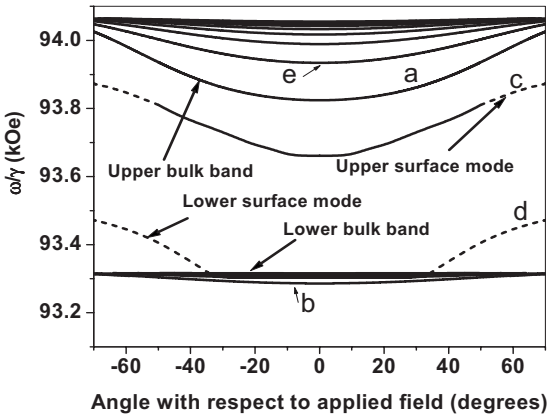


FIG. 2. Spin-wave spectrum in $MnF_2$ at thickness to wavelength ratio $q_\parallel d=4$ and $H_0=0.2$ kOe. The solid lines represent bulk modes, the dashed lines are for surface modes. The letters a-e correspond approximately to the modes examined in Fig. 3.

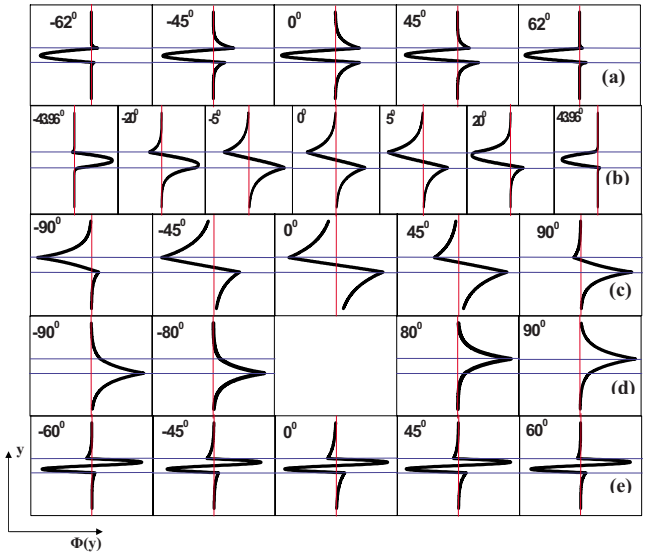


FIG. 3. (Color online) The mode pattern, i.e., the magnetic scalar potential as a function of $y$, at an applied field of 200 Oe for (a) a bulk mode in the upper bulk band region $\omega/\gamma=93.95$ kOe, (b) the lowest frequency bulk mode in lower bulk band region $\omega/\gamma=93.28$ kOe, (c) an upper surface mode at $\omega/\gamma=93.9$ kOe, (d) a lower surface mode at $\omega/\gamma=93.48$ kOe, and (e) a higher order bulk mode at $\omega/\gamma=94.05$ kOe in the upper bulk band region showing the standing wave pattern. The results are for a 1-$\mu$m-thick $MnF_2$ film.

As a first illustration we discuss the focusing phenomenon in a 1-$\mu$m-thick $MnF_2$ film in the absence of external field. Figure 4 shows the constant frequency curves and the corresponding focusing patterns for bulk modes in the upper band. In all our figures the focusing pattern is a polar plot relating the power output and the direction of observation. Here the power represents the square of the amplitude of the bulk and surface excitations at a particular frequency. The diagrams in Fig. 4 are arranged in order of increasing frequency with the largest frequency near the top of the bulk band region.

In Fig. 4(a) the constant frequency curve in the $k$ space shows some points where the curvature is small, but it never goes to zero. Hence we do not have a true caustic but still the energy is directed in six different directions. This is in contrast to the typical results on a ferromagnet where the energy was focused in either four or eight directions. Figure 4(b) is at a higher frequency. One finds that the energy focused along the $\pm z$ direction is increased compared to the Fig. 4(a) result. At an even higher frequency, near the top of the bulk band, the curvature goes through zero [see Fig. 4(c)], and there are four true caustics [compare the scales of Figs. 4(b) and 4(c)].

Now we study the effect of an external field on the focusing behavior of the bulk modes. In the presence of an external magnetic field the lower bulk band spreads over a narrow frequency range as is seen in Fig. 2. Figure 5 shows the slowness surface and the focusing pattern in the lower bulk band at a constant applied field of 200 Oe for two different frequencies. In Fig. 5(a) at $\omega/\gamma=93.28$ kOe we find that the curvature of the slowness surface goes to zero at several points and the energy is focused along 12 true caustics. Fig-

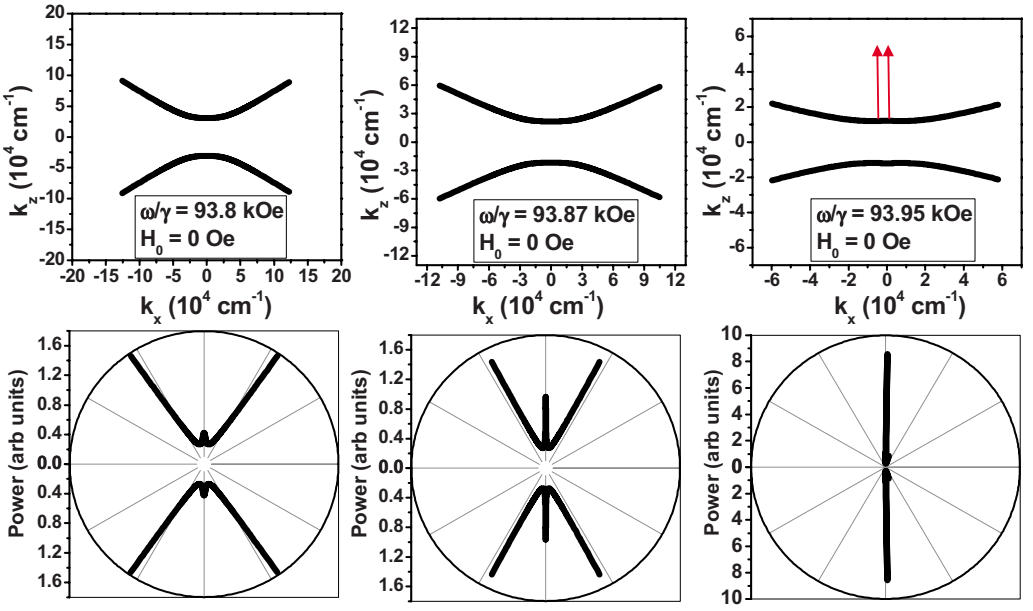


FIG. 4. (Color online) The upper panel shows the slowness surface and the lower one is the focusing pattern in the polar format for the lowest bulk mode in the upper band for 1 $\mu$m $MnF_2$ film with zero external field at (a) $\omega/\gamma$=93.8 kOe, (b) $\omega/\gamma$=93.87 kOe, and (c) $\omega/\gamma$=93.95 kOe. The arrows show the normals to the slowness surface at some of the points where the curvature is zero. The results are for a 1-$\mu$m-thick $MnF_2$ film.

ure 5(b) is at a higher frequency near the top of the lower bulk band. Again one can observe that the energy is still focused along 12 true caustics (note that some of the caustics are close to each other) but the directions are all changed from those found in Fig. 5(a). Also the focusing is slightly stronger [compare the scales in Figs. 5(a) and 5(b)] at the higher frequency near the top of the bulk band.

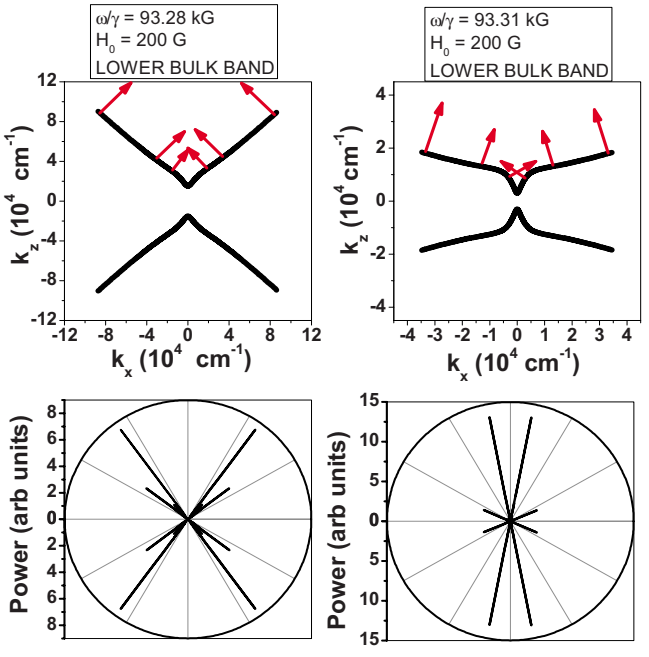


FIG. 5. (Color online) The upper panel shows the slowness surface for the lowest frequency bulk mode in the lower bulk band in $MnF_2$ at an applied field of 200 Oe at a frequency of (a) $\omega/\gamma$ =93.28 kOe and (b) $\omega/\gamma$=93.31 kOe. The lower panes show the resulting focusing pattern in a polar format. The arrows show the normals to the slowness surface at some of the points where the curvature is zero.

As noted earlier, the lower bulk band and the associated surface modes all exist in a narrow frequency band, about 100 MHz or 0.3 kOe in field units. If the frequency is held constant, say, at $\omega/\gamma$=93.28 kOe and the field is further increased then the lower bulk and surface modes are moved well below the fixed frequency. Hence to observe directional tunability with applied field, the field should be small enough so that the frequency remains within the lower bulk band.

In Fig. 6 we show the slowness surfaces and focusing patterns for the bulk modes in the upper bulk band region at an applied field of 200 Oe and at three different frequencies. The slowness surface and the focusing pattern are similar to the zero-field case (Fig. 4). One can observe that in Fig. 6(a) the curvature of the slowness surface never goes to zero and hence there are no caustics. But the curvature changes as we move along the slowness surface and hence the energy is directed along eight different directions with two directions close to each other. Figure 6(b) is at a higher frequency and one can observe that the curvature goes to zero at some points and changes at other and hence we have four true caustics along with four other directions [in Fig. 6(b), lower panel] in which the energy is focused. The lines representing the noncaustic directions are small when compared to the true caustics and are not visible on the scale of the figure. Figure 6(c) shows the slowness surface and focusing pattern at an even higher frequency near the top of the upper bulk band. The difference in the scales of Figs. 6(b) and 6(c) demonstrates that the focusing is stronger when the frequency lies near the top of the bulk band. This is consistent with our earlier results in ferromagnets.[8]

In the above focusing patterns we have fixed the magnetic field and varied the frequency of the excitation. Figure 7

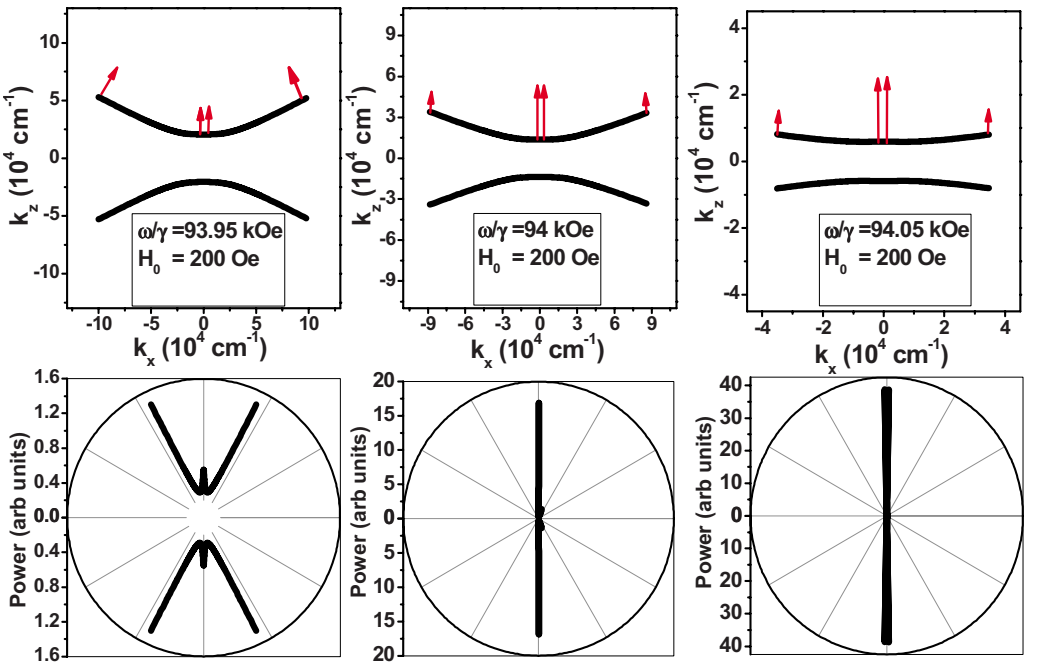


FIG. 6. (Color online) The upper panel shows the slowness surface and the lower one is the focusing pattern for the second lowest frequency bulk mode in the upper band for a one micron thick $MnF_2$ film with an external field of 200 Oe and at (a) $\omega/\gamma$=93.95 kOe, (b) $\omega/\gamma$=94 kOe and (c) $\omega/\gamma$=94.05 kOe. The lower panes show the resulting focusing pattern in a polar format. The arrows on the slowness surface show the normals to the slowness surface at some of the points where the curvature is zero.

presents results where the frequency is fixed at $\omega/\gamma$ =94.05 kOe and the applied field is varied. At an applied field of 200 Oe the frequency of 94.05 kOe is near the top of the upper bulk band frequency. In line with our earlier results one can expect true caustics at this frequency. Figure 7(a) shows a strong focusing along the applied field. If the applied field is increased, the upper bulk band is shifted up in frequency and the frequency of $\omega/\gamma$=94.05 kOe samples the bottom of the upper bulk band. Figure 7(b) shows the slowness surface and the focusing pattern for 300 Oe. Though the curvature of the slowness surface is not zero at any point, it varies along the slowness surface, and hence

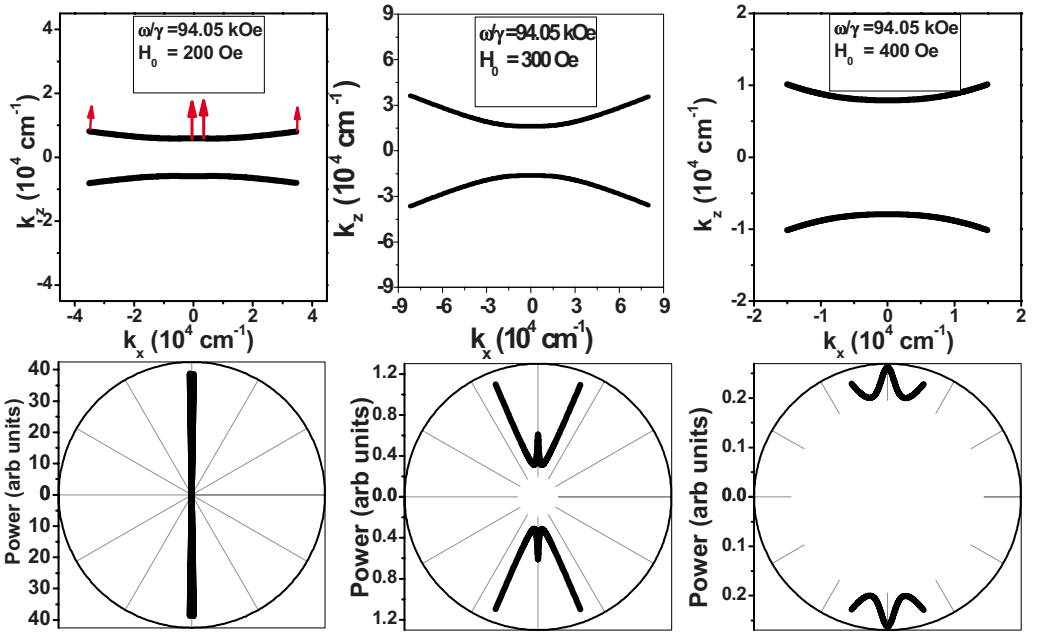


FIG. 7. (Color online) The upper panel shows the slowness surface for the second lowest frequency bulk mode in the upper bulk band for a 1-$\mu$m-thick $MnF_2$ film at a frequency of $\omega/\gamma$=94.05 kOe with an applied field of (a) 200 Oe, (b) 300 Oe, and (c) 400 Oe. The lower panes show the resulting focusing pattern in a polar format. The arrows on the slowness surface show the normals to the slowness surface at some of the points where the curvature is approaching zero. (c) is for the mixed surface/bulk mode.

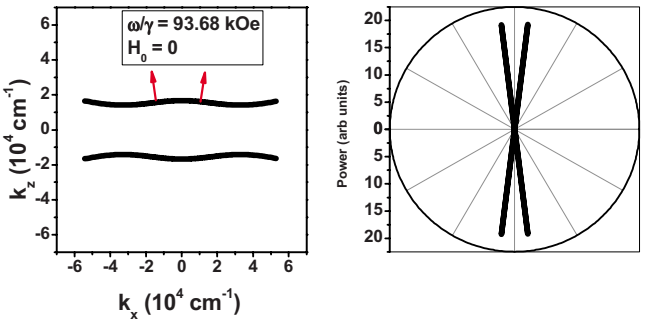


FIG. 8. (Color online) The left and right panels show the slowness surface and focusing pattern in a polar format for the surface mode in $MnF_2$ at a frequency of $\omega/\gamma=93.68$ kOe with a zero external field. (There is only one surface mode at zero field.) The arrows on the slowness surface show the normals to the slowness surface at some of the points where the curvature is zero.

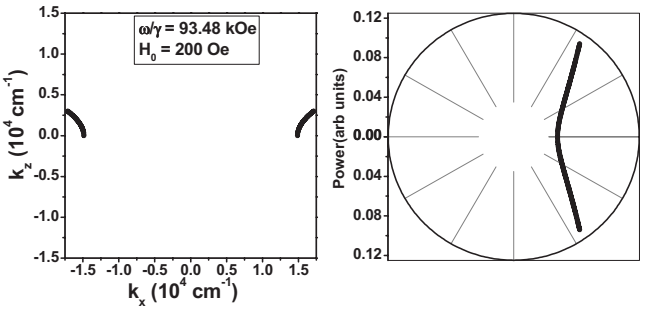


FIG. 9. The left and right panels show the slowness surface and focusing pattern in a polar format for the surface mode in $MnF_2$ at a frequency of $\omega/\gamma=93.48$ kOe (in the lower band) with a 200 Oe external field.

there are some particular directions in which more energy is focused. As we increase the field more, we find that the constant frequency of $\omega/\gamma=94.05$ kOe moves to the bottom of the bulk band and Fig. 7(c) represents the upper surface mode which lies in between the lower and upper bulk bands. One can easily observe that the curvature is never zero and hence we cannot get a caustic. However, the change in the curvature focuses more energy in particular directions.

As discussed earlier, one interesting feature in the antiferromagnetic film is that there are *two* magnetostatic surface modes with different frequencies. In Fig. 8 we have shown the slowness surface and the focusing pattern for the lower frequency surface mode in zero field. The slowness surface has an interesting pattern where the curvature goes to zero at several points and hence they exhibit true caustics. This is in contrast to a ferromagnetic film where the magnetostatic surface modes show only weak focusing.[8]

In the presence of applied field the surface modes are well separated and the lower surface mode merges with the lower bulk band at some critical angles.[15] Figure 9 shows the slowness surface and the focusing pattern of the surface mode near the lower bulk band. The slowness surface is restricted to some $k_x$ value where it merges with the bulk band. Unlike the $H=0$ case, the curvature is never zero and there are no true caustics. However, there is some weak focusing due to the changes in curvature along the slowness surface.

Figure 10 shows the surface mode near the upper bulk band region at a constant frequency of $\omega/\gamma=93.9$ kOe for different applied fields. As seen in Fig. 2, these surface modes change into bulk modes at some particular angle of propagation. Nonetheless, one may still find a focusing pattern for this mode in the usual way. Figure 10(a) shows the slowness surface and focusing pattern for an applied field of 200 Oe. At this field, there are no caustics for this mode; instead the energy is focused in particular directions due to the changes in the curvature found along the slowness sur-

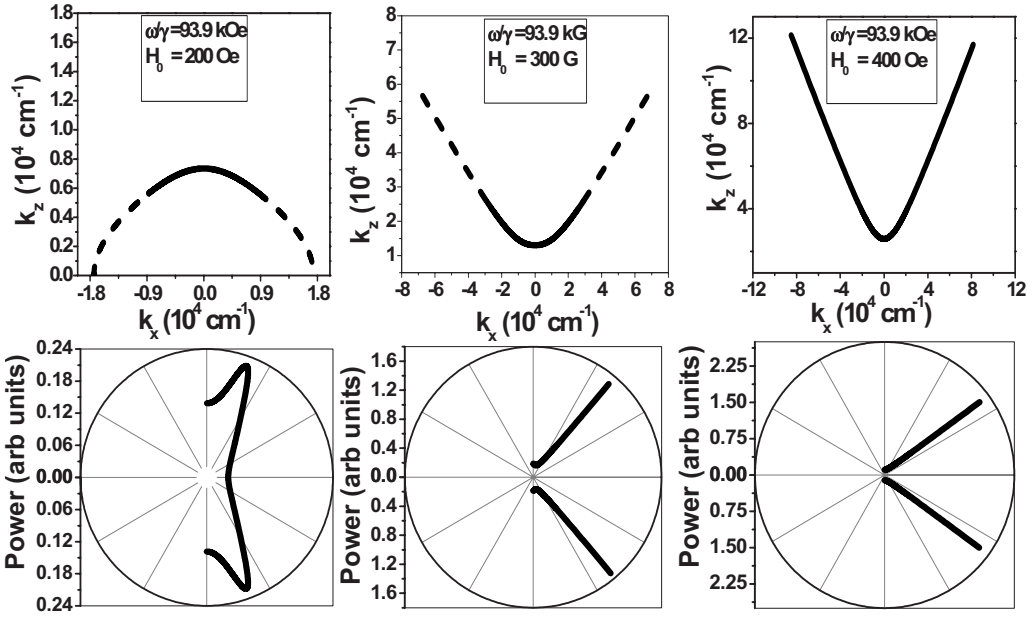


FIG. 10. The upper panel shows the slowness surface for the upper bulk/surface mode in $MnF_2$ at a frequency of $\omega/\gamma=93.9$ kOe with an applied field of (a) 200 Oe, (b) 300 Oe, and (c) 400 Oe. The lower panels show the resulting focusing pattern in a polar format. The upper panels of (a) and (b) are composed of bulk mode excitations (solid line) and a surface excitation (dotted line).

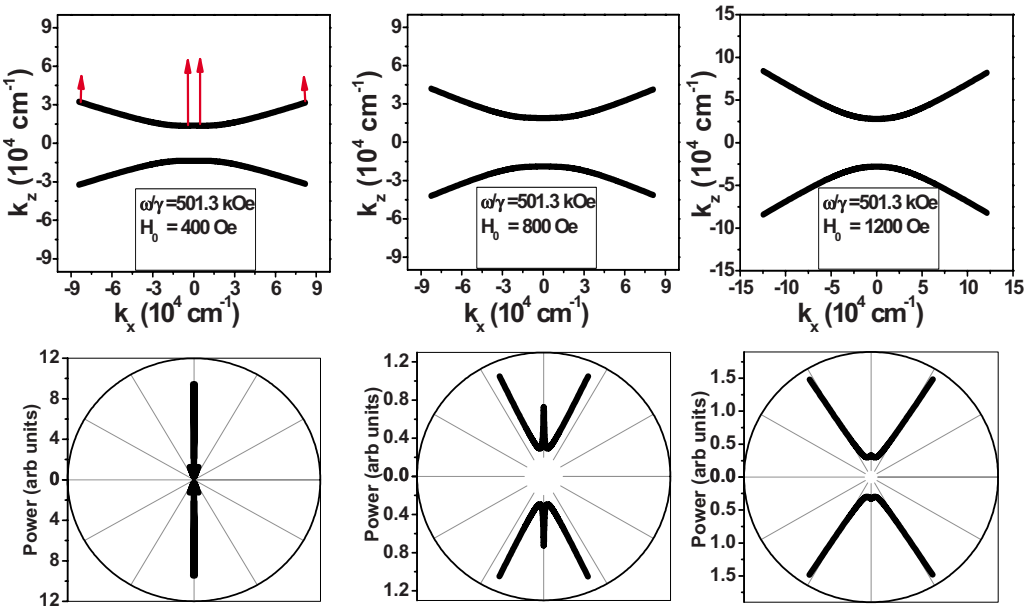


FIG. 11. (Color online) The upper panel shows the slowness surface for a surface mode in $FeF_2$ at a frequency of $\omega/\gamma=501.3$ kOe with an applied field of (a) 400 Oe, (b) 800 Oe, and (c) 1200 Oe. The lower panels show the resulting focusing pattern in a polar format.

face. Figure 10(b) shows the focusing results for an external field of 300 Oe where the surface character of the mode is still observed and the focusing of energy is stronger when compared to the low-field case. In Fig. 10(c) at an applied field of 400 Oe, we find a bulk mode instead of a surface mode at the frequency $\omega/\gamma=93.9$ kOe. In essence the increase in the field has moved the upper band of modes in Fig. 2 up in frequency so that $\omega/\gamma=93.9$ kOe now intersects a bulk mode. The focusing pattern at the external field of 400 Oe is now similar to that of a bulk mode near the bottom of the bulk spin-wave band. The focusing seen in Figs. 10(b) and 10(c) do not appear to be true caustics, but the curvature in the slowness surfaces is very close to zero at some points.

In order to study the effect of the exchange field and the anisotropy field on the focusing behavior of bulk and surface modes we have examined different antiferromagnetic materials $FeF_2$ and $GdAlO_3$. $FeF_2$ has high anisotropy and exchange fields compared to $MnF_2$ while $GdAlO_3$ has weaker anisotropy and exchange fields. An example of focusing in $FeF_2$ is shown in Fig. 11 for a frequency of 501.3 kOe and external fields of 0.4, 0.8, and 1.2 kOe. The general features of the focusing behavior are similar to that found in $MnF_2$ except that the frequency of operation is different, about 36 GHz for $GdAlO_3$ and about 1.1 THz for $FeF_2$. Since the focusing can be adjusted by tuning the frequency and the applied field this idea can be used for a tunable filter in a range of frequencies, from about 50 GHz to 1 THz, depending on the choice of the antiferromagnetic material. We note that magnetic bulk and surface modes in $FeF_2$ have been probed using reflectivity and attenuated total reflectivity measurements with good agreement between experiment and theory.[21–23]

The present study can lead to a new practical application in signal processing. The ability to efficiently steer or route signals in an adaptive or dynamic fashion is very important in high-frequency signal processing. In this paper we have shown the feasibility of a device which we call a high-frequency router. Such a device can separate high-frequency signals and send them in different directions, controlled by the frequency of the signal and the magnitude of the external field. This is clearly shown in our results in Figs. 4–11. In order to explain this phenomenon we choose, as an example, Fig. 5, which shows the focusing of the bulk waves at $\omega/\gamma=93.28$ kOe and $\omega/\gamma=93.31$ kOe for an applied field of 200 Oe. The focusing pattern clearly shows that the two waves are routed in two different directions. The routing of the waves at the frequencies $\omega/\gamma=93.28$ kOe and $\omega/\gamma=93.31$ kOe is possible at an applied field near 200 Oe. As the applied field is changed, the frequency spectrum will be different and hence there will be routing of waves at different frequencies. This is clearly shown in Fig. 7 for the second lowest frequency bulk mode in the upper bulk band. Thus by either changing the frequency or the applied field we can achieve routing of the waves into different directions. Our study shows that it is possible, with very thin films in the order of 1 $\mu$m, to obtain well-distinguishable waves of different frequencies at the output, thus realizing the desired routing function which is tunable with applied field and frequency

## IV. CONCLUSIONS AND DISCUSSION

In this paper we have investigated the focusing of magnetostatic bulk and surface waves in antiferromagnetic thin films. We use a 1-$\mu$m-thick $MnF_2$ film as our primary example. The study is carried out by finding the slowness surface for different frequencies and magnitudes of applied field. This is done by solving the implicit dispersion relation numerically, and from the slowness surface we have found the focusing pattern by calculating the curvature at every point on it. In contrast to modes found in a ferromagnet, antiferromagnets show bulk and surface modes in zero field

and in the presence of an external field the bulk mode splits into a lower and upper bulk bands with surface modes connected to both lower and upper bands.

In general our study shows that bulk modes at the bottom of the lower bulk band are focused strongly compared to those at the bottom of the upper bulk band. Our earlier studies on ferromagnets and our present study have shown that the number of focusing directions increases as we move the driving frequency up toward the top of the bulk band.

In contrast to the magnetostatic surface modes in the ferromagnet, the surface modes in antiferromagnet are focused relatively strongly. We have observed that the focusing directions can be changed by altering the magnitude of the applied field. Since different fields cause the energy to be focused into different directions we can use this idea to make tunable filters. Furthermore, at a given field different frequencies are focused in different directions. We have pointed out that this idea can be used to build a high-frequency router that separates frequencies into different directions in the microwave or millimeter frequency range.

The study of effect of exchange interaction on the focusing of the spin waves in antiferromagnetic thin films is a bit tedious mathematically,[16] and we have left that for future investigation.

## ACKNOWLEDGMENTS

This work was supported by DOA under Grant No. W911NF-04-1-0247.

[1] V. T. Buchwald, Proc. R. Soc. London, Ser. A **253**, 563 (1959).
[2] B. Taylor, H. J. Maris, and C. Elbaum, Phys. Rev. Lett. **23**, 416 (1969); Phys. Rev. B **3**, 1462 (1971).
[3] P. Taborek and D. Goodstein, Solid State Commun. **33**, 1191 (1980).
[4] V. T. Buchwald, Q. J. Mech. Appl. Math. **14**, 293 (1961); V. T. Buchwald and A. Davis, *ibid.* **16**, 283 (1963).
[5] G. A. Northrop and J. P. Wolfe, Phys. Rev. Lett. **43**, 1424 (1979).
[6] G. A. Northrop and J. P. Wolfe, Phys. Rev. B **22**, 6196 (1980).
[7] R. E. Camley and A. A. Maradudin, Phys. Rev. B **27**, 1959 (1983).
[8] V. Veerakumar and R. E. Camley, Phys. Rev. B **74**, 214401 (2006).
[9] T. Schneider, A. A. Serga, A. V. Chumak, C. W. Sandweg, S. Trudel, S. Wolff, M. P. Kostylev, V. S. Tiberkevich, A. N. Slavin, and B. Hillebrands, Phys. Rev. Lett. **104**, 197203 (2010).
[10] V. E. Demidov, S. O. Demokritov, D. Birt, B. O'Gorman, M. Tsoi, and X. Li, Phys. Rev. B **80**, 014429 (2009).
[11] R. Loudon and P. Pincus, Phys. Rev. **132**, 673 (1963).
[12] D. E. Beeman, J. Appl. Phys. **37**, 1136 (1966).
[13] J. P. Kotthaus and V. Jaccarino, Phys. Rev. Lett. **28**, 1649 (1972).
[14] R. E. Camley, Phys. Rev. Lett. **45**, 283 (1980).
[15] R. L. Stamps and R. E. Camley, J. Appl. Phys. **56**, 3497 (1984).
[16] R. L. Stamps and R. E. Camley, Phys. Rev. B **35**, 1919 (1987).
[17] M. G. Cottam and D. R. Tilley, *Introduction to Surface and Superlattice Excitations* (Cambridge University Press, Cambridge, 1989).
[18] L. R. Walker, Phys. Rev. **105**, 390 (1957); J. Appl. Phys. **29**, 318 (1958).
[19] A. R. King, V. Jaccarino, and S. M. Rezende, Phys. Rev. Lett. **37**, 533 (1976).
[20] K. W. Blazey, H. Rohrer, and R. Webster, Phys. Rev. B **4**, 2287 (1971).
[21] M. R. F. Jensen, S. A. Feiven, T. J. Parker, and R. E. Camley, J. Phys.: Condens. Matter **9**, 7233 (1997).
[22] R. E. Camley, M. R. F. Jensen, S. A. Feiven, and T. J. Parker, J. Appl. Phys. **83**, 6280 (1998) and references therein.
[23] M. R. F. Jensen, T. J. Parker, Kamsul Abraha, and D. R. Tilley, Phys. Rev. Lett. **75**, 3756 (1995).